Phase scaling properties of perturbation-induced multistability in a driven nonlinear system

V. N. Chizhevsky[1,*] and R. Corbalán[2]
[1]*B. I. Stepanov Institute of Physics, National Academy of Science of Belarus, 220072 Minsk, Belarus*
[2]*Departament de Física, Universitat Autònoma de Barcelona, E-08193 Bellaterra (Barcelona), Spain*
(Received 19 November 2001; published 8 July 2002)

Phase scaling relations for the onsets of both saddle-node bifurcations and boundary crises induced by resonant periodic perturbations at subharmonic frequencies are found in a period-doubled system from the results of numerical simulation. These phase dependences determine the domains of existence of induced attractors in (bifurcation parameter, perturbation phase) parameter space. The overlapping of these domains leads to the formation of zones with different numbers of coexisting attractors. The numerical evidence was obtained on the basis of single-mode rate equations of a laser with parameters corresponding to a realistic loss-modulated CO_2 laser.

DOI: 10.1103/PhysRevE.66.016201 PACS number(s): 05.45.Pq, 42.65.Sf, 42.55.Lt

The response of driven nonlinear systems to the effect of a resonant periodic perturbation is known to be very sensitive to the phase difference between driving and perturbation frequencies. Specifically, phase effects have been found in the nonfeedback control of chaos [1–6], small signal amplification and classical squeezing near the first period-doubling bifurcation [7,8], trajectory selection in multistable systems [9,10], stabilization and destabilization of periodic orbits (the phase control of dynamical systems) [5], the bistability induced by the periodic perturbation at the first subharmonic frequency [11,12], unfolding of the period-2 pitchfork bifurcation [13], and the resonant goal-oriented control of nonautonomous systems [14]. It was also found that a change in the phase of the resonant perturbation leads to global changes in full bifurcation diagrams [15].

Recently, it was experimentally and numerically shown that the resonant perturbation at the frequency f_d/n (where f_d is the main driving frequency, $n=2,4,8,16,\ldots$) can induce in period-doubled systems up to n coexisting attractors via the mechanism of a so-called imperfect bifurcation. The experimental and numerical evidence was obtained on the basis of a loss-modulated CO_2 laser [16]. Although all results presented there were obtained with the zero phase of the resonant perturbation, it was also mentioned that the phase of the resonant perturbation can play an important role in obtaining multistability in the sense that a change in the phase may result in a change of the number of attractors induced.

This paper is directly devoted to a detailed numerical study of phase effects in the multistability induced by resonant perturbations using the well known single-mode laser equations [17]. As shown in Ref. [16], the location of attractors induced by resonant perturbations on the bifurcation diagrams is determined by two critical points: saddle-node bifurcations and boundary crises at which new attractors appear and disappear, respectively, as a bifurcation parameter increases. Therefore, we studied the dependences of these critical points on the perturbation phase. Based on the results of the numerical simulation, phase scaling laws relating the onset of saddle-node bifurcations induced by the resonant perturbation at the frequencies $f_d/n(n=2,4,8)$ with their phases were found in the vicinity of the first three originally unperturbed period-doubling bifurcations. In addition, the scaling laws relating the perturbation phase and the critical value of the bifurcation parameter for the boundary crisis induced by weak periodic perturbations were also found. For both types of critical point we present a generalization of the effect of the phase of the resonant periodic perturbation with an arbitrary subharmonic frequency f_d/n. Such phase dependences lead to an interesting consequence: for certain values of the bifurcation parameter, by varying the perturbation phase monotonically, we can periodically change the number of coexisting attractors.

The phase effects for the perturbation-induced multistability were studied numerically, as in Ref. [16], with the help of the bifurcation diagrams in the presence of resonant perturbations using the well known single-mode laser equations [17]

$$\frac{du}{dt}=\tau^{-1}(y-k)u, \tag{1}$$

$$\frac{dy}{dt}=(y_0-y)\gamma-uy,$$

where

$$k=k_0+k_d\cos(2\pi f_d t)+k_p\cos(2\pi f_d t/n+\varphi). \tag{2}$$

Here u is proportional to the radiation density, y and y_0 are the gain and the unsaturated gain in the active medium, respectively, τ is the transit time of light in the cavity, γ is the gain decay rate, k is the total cavity loss, k_0 is the constant part of the loss, k_d is the driving amplitude, k_p is the perturbation amplitude, f_d is the driving frequency, φ is the perturbation phase, and $n=2,4,8,\ldots$. Throughout the calculations the following fixed parameters were used: $\tau=3.5\times10^{-9}$ s, $\gamma=1.978\times10^{5}$ s^{-1}, $y_0=0.175$, $k_0=0.1731$. The relaxation oscillation of the laser was $f_{ro}=50$ kHz and the driving frequency was $f_d=100$ kHz. All these parameters correspond to a realistic CO_2 laser. In the numerical simulations two parameters k_d and φ were varied. Hereafter,

*Electronic address: vnc@dragon.bas-net.by

the normalized bifurcation parameter μ and the perturbation amplitude ε are used (defined as $\mu = k_d/k_1$ and $\varepsilon = k_p/k_1$, respectively, where $k_1 = 2.478 \times 10^{-3}$ is the first period-doubling threshold in the absence of the perturbation). The amplitude of the loss perturbations k_p was taken so that the values of ε would be small.

Let us consider in series the influence of the phase of the perturbations with frequencies $f_d/2$, $f_d/4$, and $f_d/8$ on the first three period-doubling bifurcations and the last three band-merging crises. This consideration will allow us then to make a generalization of the effect of the perturbation phase for an arbitrary subharmonic frequency.

(i) Phase effects in the presence of a resonant perturbation with a frequency $f_d/2$. Some aspects of this problem were investigated numerically and experimentally in [11–13,15], mainly in the vicinity of the first period-doubling bifurcation. From these investigations, we note the results obtained by Newell *et al.* [13], which are relevant to our study. Using a specific mapping, derived from single-mode laser equations, relating the amplitude of spikes and the interspike intervals, they found that the resonant perturbation at the frequency $f_d/2$ destroys the period-2 pitchfork bifurcation, which is replaced by a smooth transition branch and a new fixed point. They found that the phase dependence of the location of this limit point is proportional to $\cos^{2/3}(\varphi)$, where φ is the phase of the resonant perturbation. Further, we will show that similar phase dependences occur for all saddle-node bifurcations which appear in the vicinity of the original period-doubling bifurcations in the presence of the resonant periodic perturbations.

Figure 1 shows bifurcation diagrams of the laser in the presence of a perturbation at $f_d/2$ with two different phases. These bifurcation diagrams were obtained by a superimposition of several generated with randomly distributed initial conditions. For reference, Fig. 1(a) shows the bifurcation diagram of the laser without perturbation. Figures 1(b) and 1(c) correspond to the effect of the perturbation with phases $\varphi = \pi/6$ and $\varphi = 2\pi/3$, respectively. In order to simplify these two last diagrams, only one subband of each attractor is shown in Figs. 1(b) and 1(c). One can see on both figures that a coexistence of two attractors can be found between two critical points, the locations of which are strongly phase dependent: μ_{sn}, where the second attractor appears via a saddle-node bifurcation, and μ_{bc}, where the first (or the second) attractor disappears through a boundary crisis. The phase dependence of the location of these critical points (μ_{sn} and μ_{bc}) in (μ, φ) parameter space is shown in Figs. 2(a) and 2(b), respectively. The fitting of the numerical data gives the following scaling law which relates μ_{sn} and the perturbation phase φ in the vicinity of the original first period-doubling bifurcation μ_1:

$$\mu_{sn} \approx \mu_1 + A|\cos^{\alpha}(\varphi + \varphi_{sn}^0)|, \tag{3}$$

where A is a coefficient that depends on the perturbation amplitude ε, and $\varphi_{sn}^0 \approx 61.35°$ is the initial phase shift, which is determined by the dissipation in the laser. For the given $\varepsilon = 3.53 \times 10^{-3}$ used in the simulation we obtained $A \approx 0.091$. In this case the fitting of the numerical data gives

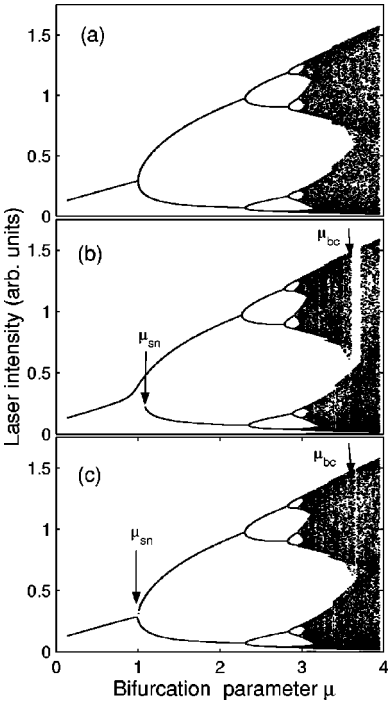

FIG. 1. The bifurcation diagrams of the laser versus μ in the absence (a) and in the presence of a resonant perturbation at frequency $f_d/2$ with two different phases $\varphi = \pi/6$ (b) and $\varphi = 2\pi/3$ (c). μ_{sn} and μ_{bc} denote critical values corresponding to the appearance of the saddle-node bifurcation and boundary crisis, respectively, induced by the perturbation at $f_d/2$. The perturbation amplitude $\epsilon = 3.53 \times 10^{-3}$.

$\alpha \approx 0.67$, which is very close to the value 2/3 predicted in Ref. [13] from the class *B* laser map. Therefore, we can assign $\alpha \approx 2/3$ with a rather high accuracy. Obviously, there exist values of the phase for which the effect of the resonant perturbation can be both minimal ($\varphi_{\min} \approx 28.65°$) and maximal ($\varphi_{\max} \approx 118.65°$) in the sense of the distance between the saddle-node bifurcation induced and the original period-doubling bifurcation.

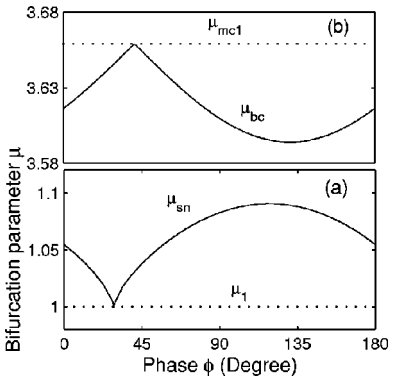

FIG. 2. Phase dependences of critical values for the onset of (a) saddle-node bifurcation μ_{sn} and (b) boundary crisis μ_{bc} induced by resonant perturbations at frequency $f_d/2$. μ_1 and μ_{mc1} denote critical values for the first period-doubling bifurcation and the last band-merging crisis in the absence of the resonant perturbation. The perturbation amplitude $\epsilon = 3.53 \times 10^{-3}$.

An analogous scaling law, but with a different exponent, is obtained for the phase dependence of the critical value for the boundary crisis μ_{bc}:

$$\mu_{bc} \approx \mu_{mc} - B|\cos^{\beta}(\varphi + \varphi_{bc}^{0})|, \tag{4}$$

where $\mu_{mc} \approx 3.6598$ is the value of the bifurcation parameter corresponding to the last band-merging crisis in the absence of the resonant perturbation, B is a coefficient (in our case for the $\varepsilon = 3.53 \times 10^{-3}$ used in the simulation we obtained $B \approx 0.0917$) and $\varphi_{bc}^{0} \approx 49.04°$ is the initial phase shift. For small values of ε, the fitting of the numerical data yields $\beta \approx 1$. It should be noted that the strong influence of the phase of the second resonant modulation on the boundary and internal crises was pointed out in Ref. [15], although they have not found any simple relation between dephasing φ and the location of the critical points for crises. For the given perturbation amplitude ε, these curves (μ_{sn} and μ_{bc}) in (μ, φ) parameter space serve as boundaries of zones with different numbers of attractors. Below the curve μ_{sn} there is only one attractor, between curves μ_{sn} and μ_{bc} there are two coexisting attractors, and above the curve μ_{bc} we have again one attractor. For given ε and certain ranges of μ, by varying only the phase, we can periodically change the number of attractors between 1 and 2, which can be either in the periodic or in a chaotic state.

(ii) Phase effects in the presence of a resonant perturbation with frequency $f_d/4$. Figure 3 shows bifurcation diagrams of the laser in the presence of a perturbation at $f_d/4$ with three different phases $\varphi = \pi/6$ [Fig. 3(a)], $\varphi = \pi/3$ [Fig. 3(b)], and $\varphi = 4\pi/9$ [Fig. 3(c)] which were obtained by the same procedure mentioned above. As in the previous case only one subband from four for each attractor is shown in the figures. For a certain range of the bifurcation parameter, such a perturbation can induce four attractors, which one can see on each diagram of Fig. 3. The second attractor appears just above the first original period-doubling bifurcation (this range of μ is not shown in Fig. 3), and the third and fourth appear above the second period-doubling bifurcation. Comparing the diagrams in Fig. 3 one can see that the relative positions of all attractors and correspondingly all bifurcation points associated with them strongly depend on the phase of the resonant perturbation. Figure 4 summarizes the influence of the phase on the location of all saddle-node bifurcations and critical points for boundary crises induced by a perturbation at frequency $f_d/4$ in the vicinity of the original first [Fig. 4(a)] and second [Fig. 4(b)] period-doubling bifurcations and, correspondingly, near the original last [Fig. 4(c)] and penultimate [Fig. 4(d)] band-merging crises. The phase dependence for the location of the saddle-node bifurcation μ_{sn1} in the vicinity of the first period-doubling bifurcation, represented in Fig. 4(a), can be approximated by the following expression:

$$\mu_{sn1} \approx \mu_1 + A|\cos^{\alpha}(2\varphi + \varphi_{sn1}^{0})|, \tag{5}$$

where $A \approx 1.1 \times 10^{-3}$ (for $\varepsilon = 1.41 \times 10^{-3}$ used in the simulation), and $\varphi_{sn1}^{0} \approx 3.52°$. The fitting of the numerical data yields $\alpha \approx 2/3$. Comparing expressions (3) and (5) one can see that this relation has phase-doubled dependence. The second peculiarity is that the effect of the resonant perturbation at the frequency $f_d/4$ on the first period-doubling bifurcation is very small.

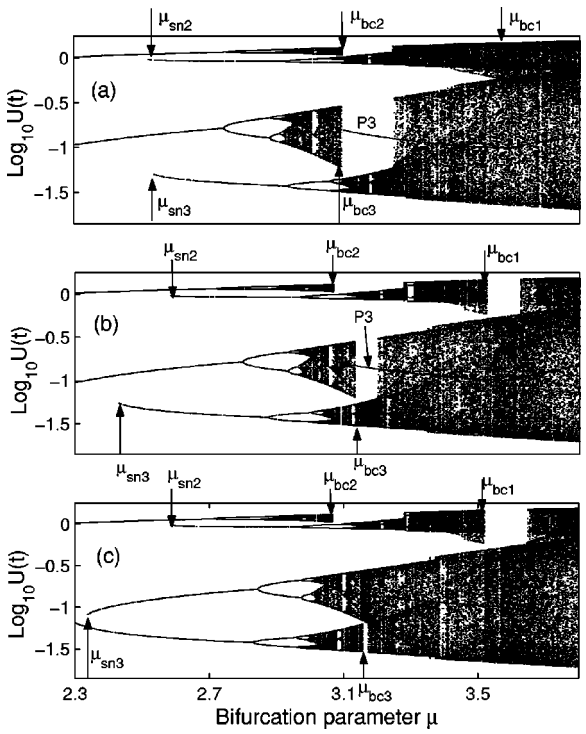

FIG. 3. The bifurcation diagrams of the laser versus μ in the presence of a resonant perturbation at frequency $f_d/4$ with three different phases (a) $\varphi = \pi/6$, (b) $\varphi = \pi/3$, and (c) $\varphi = 4\pi/9$. μ_{sni} and μ_{bci} $(i = 1,2,3)$ denote critical values corresponding to the appearance of saddle-node bifurcations and boundary crises, respectively. $P3$ denotes a period-3 branch which appears at $\mu \approx 3.065$. The perturbation amplitude $\epsilon = 1.41 \times 10^{-3}$.

The phase dependences for the location of saddle-node bifurcations (μ_{sn2} and μ_{sn3}) in the vicinity of the second period-doubling bifurcation, shown in Fig. 4(b), can be approximated by the expression (3), where μ_1 should be replaced by μ_2 (μ_2 is the threshold value for the second period-doubling bifurcation); φ_{sn}^{0} is an initial phase shift which is different for the two curves and differing by $\pi/2$. This means there are two curves which are shifted by $\pi/2$ with respect to each other. For a small value of ε, the fitting of the numerical data yields $\alpha \approx 2/3$ for both curves.

A similar situation takes place in the vicinity of the two last band-merging crises. Near the penultimate one we have two boundary crises [denoted in Fig. 4(c) as μ_{bc3} and μ_{bc2}], the location of which can be approximated by expression (4), where μ_{mc1} should be replaced by μ_{mc2} (μ_2 is the threshold value for the penultimate band-merging crisis); φ_{bc}^{0}, as in the previous case, is different for the two curves and differs by $\pi/2$. Therefore, there are again two $\pi/2$-shifted curves. The fitting of the numerical data gives $\beta \approx 1$ which coincides with the previous case for the boundary crisis represented in Fig. 2(b). In what follows, the numbering of band-merging crises will here be in the reverse order, so that the last one is denoted as μ_{mc1}, the penultimate one as μ_{mc2}, and so on up to the accumulation point.

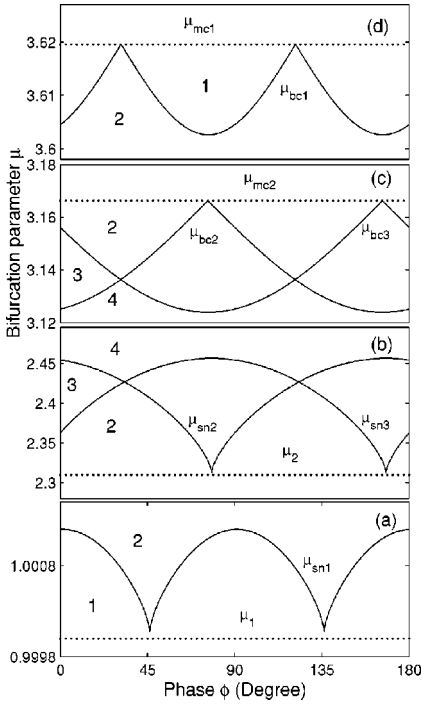

FIG. 4. Phase dependences of critical values for the onset of (a) saddle-node bifurcations μ_{sni}, and (b) boundary crisis μ_{bci} ($i=1,2,3$) induced by resonant perturbations at frequency $f_d/4$. μ_i and μ_{mci} correspond to normalized threshold values for period-doubling bifurcations and band-merging crises in the absence of the resonant perturbation. The perturbation amplitude $\epsilon=1.41\times10^{-3}$. The numbers on the figure denote the number of attractors in every zone.

In the vicinity of the last band-merging crisis (μ_{mc1}) the phase dependence for the boundary crisis [denoted in Fig. 4(d) as μ_{bc1}] can be expressed as

$$\mu_{bc1}\approx\mu_{mc1}-B|\cos^{\beta}(2\varphi+\varphi^0_{bc1})|, \tag{6}$$

where $\mu_{mc1}\approx3.6598$,$\varphi^0_{bc1}\approx27.42°$, and $B\approx1.69\times10^{-2}$ (for $\varepsilon\approx1.41\times10^{-3}$ used in the simulation). The fitting of the data yields again $\beta\approx1$ as in the previous case for the boundary crisis.

The intersection of these curves leads to the formation of zones with different numbers of attractors. The numbers on the figure denote the number of attractors in every zone. This means that for a given ε, by varying the perturbation phase φ and depending on the value of the bifurcation parameter μ, we can change the number of attractors between 1 and 2, 2 and 3, 3 and 4. There are some values of the phase at which two attractors appear and disappear simultaneously, but these values of the phase are different for saddle-node bifurcations and boundary crises.

(iii) Phase effects in the presence of a resonant perturbation with frequency $f_d/8$. We consider this case in order to generalize the effect of the phase of the resonant perturbation with higher-order subharmonic frequencies. It should be noted that this case repeats all regularities found in the preceding case; therefore we shall consider it very briefly. Figure 5 shows the phase dependences for this case in the vicinity of the first three original period-doubling bifurcations

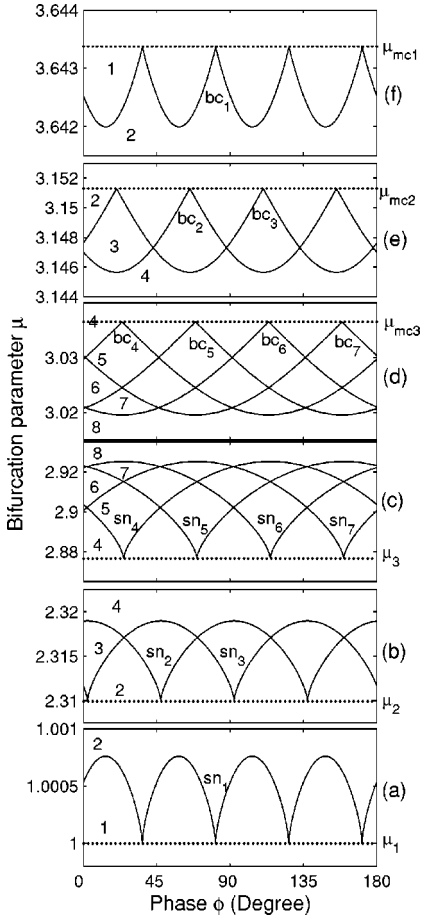

FIG. 5. Phase dependences of critical values for the onset of (a) saddle-node bifurcations μ_{sni} and (b) boundary crises μ_{bci} ($i=1,2,\ldots,7$) induced by resonant perturbations at frequency $f_d/8$. The perturbation amplitude $\epsilon=0.706\times10^{-3}$. The numbers on the figure denote the number of attractors in every zone.

[Figs. 5(a)–5(c)] and near the last three original band-merging crises [Figs. 5(d)–5(f)]. Above the first period-doubling bifurcation [Fig. 5(a)] we have again the phase-doubled dependence with respect to the previous case represented in Fig. 4(a). In the vicinity of the second period-doubling bifurcation there are two $\pi/2$-shifted phase-doubled dependences [Fig. 5(b)], and above the third period-doubling bifurcation there exist four phase dependences for saddle-node bifurcations shifted by $\pi/4$ with respect to each other [Fig. 5(c)]. A similar picture, but in reverse order, is observed for the phase effects of boundary crises in the vicinity of the last three band-merging crises which are represented in Figs. 5(d)–5(f). For the given $\varepsilon\approx0.706\times10^{-3}$, the fitting of the numerical data yields $\alpha\approx2/3$ for all saddle-node bifurcations and $\beta\approx1$ for all boundary crises represented in Fig. 5.

Taking into account all regularities found previously, for the given perturbation amplitude ε we can write a general relation that allows one to find the phase dependence of any saddle-node bifurcation and critical point for a boundary crisis induced by weak resonant perturbations with an arbitrary subharmonic frequency $f_d/2^k$ ($k=1,2,3,\ldots$). The phase dependence for the onset of the jth saddle-node bifurcation induced by a resonant perturbation at frequency $f_d/2^k$ in the

vicinity of the ith initial period-doubling bifurcation can be expressed as

$$\mu_{i,j}^{sn} \approx \mu_i^{pd} + A_i |\cos^{\alpha}[2^{k-i}\varphi + \pi(j-1)/2^{i-1} + \varphi_{0i}^{sn})| \quad (7)$$

$$(i = 1,2,\ldots,k \text{ and } j = 1,2,\ldots,2^{i-1}),$$

where μ_i^{pd} is the value of the bifurcation parameter μ corresponding to the ith period-doubling bifurcation in the absence of the resonant perturbation, A_i is the corresponding coefficient, which depends on the value of ε, and φ_{0i}^{sn} is the initial phase shift, which is different for different i. In general, α depends on ε, but for small ε we can assign $\alpha \approx 2/3$.

A similar phase dependence occurs for the critical values for boundary crises:

$$\mu_{i,j}^{bc} \approx \mu_i^{mc} - B_i |\cos^{\beta}[2^{k-i}\varphi + \pi(j-1)/2^{i-1} + \varphi_{0i}^{bc}]| \quad (8)$$

$$(i = 1,2,\ldots,k \text{ and } j = 1,2,\ldots,2^{i-1}),$$

where μ_i^{mc} is the critical value corresponding to the ith unperturbed band-merging crisis, B_i is a coefficient, and φ_{0i}^{bc} is the initial phase shift, both of which are different for different i. Taking into account all previously studied cases, we can assign $\beta \approx 1$ for small values of ε. It should be noted that with increasing ε both exponents α and β also increase. Obviously, these curves in (μ,φ) parameter space can be considered as boundaries of domains of existence of different attractors. The overlapping of these domains results in the appearance of multistable states, the number of which for a given perturbation amplitude ε depends on the bifurcation parameter μ and the perturbation phase φ as shown in Figs. 4 and 5.

To conclude, we have found from a numerical simulation of a loss-modulated CO_2 laser simple phase scaling relations for the location of both saddle-node bifurcations and boundary crises induced by resonant perturbations at subharmonic frequencies. For a given perturbation amplitude these phase dependences allow one to find zones with different numbers of coexisting attractors in (bifurcation parameter, perturbation phase) parameter space. Since the period-doubling cascade is a universal feature of driven nonlinear systems one can expect that analogous phase properties will be observed in many other systems in the presence of resonant periodic perturbations at subharmonic frequencies.

Partial financial support from the DGESIC (Spain), through Project No. PB98-0935-C03-03 is gratefully acknowledged.

[1] L. Fronzoni, M. Giocondo, and M. Pettini, Phys. Rev. A **43**, 6483 (1991).
[2] R. Meucci, W. Gadomski, M. Ciofini, and F.T. Arecchi, Phys. Rev. E **49**, R2528 (1994).
[3] Z. Qu, G. Hu, G. Yang, and G. Qin, Phys. Rev. Lett. **74**, 1736 (1995).
[4] J. Yang, Zhilin Qu, and G. Hu, Phys. Rev. E **53**, 4402 (1996).
[5] V.N. Chizhevsky and R. Corbalán, Phys. Rev. E **54**, 4576 (1996).
[6] R. Chacon, Phys. Rev. Lett. **77**, 482 (1996); *ibid.* **86**, 1737 (2001).
[7] R. Corbalán, J. Cortit, A.N. Pisarchik, V.N. Chizhevsky, and R. Vilaseca, Phys. Rev. A **51**, 663 (1995); R. Corbalán, J. Cortit, V.N. Chizhevsky, and A.N. Pisarchik, Infrared Phys. Technol. **36**, 71 (1995).
[8] P. Glorieux, C. Lepers, R. Corbalán, J. Cortit, and A.N. Pisarchik, Opt. Commun. **118**, 309 (1995).
[9] W. Yang, M. Ding, and H. Gang, Phys. Rev. Lett. **74**, 3955 (1995).
[10] Y. Jiang, Phys. Lett. A **264**, 22 (1999).
[11] V.N. Chizhevsky, R. Corbalán, and A.N. Pisarchik, Phys. Rev. E **56**, 1580 (1997).
[12] V.N. Chizhevsky, R. Vilaseca, and R. Corbalán, Int. J. Bifurcation Chaos Appl. Sci. Eng. **8**, 1777 (1998).
[13] T.C. Newell, A. Gavrielides, D. Sukow, V. Kovanis, T. Erneux, and S.A. Glasgow, Phys. Rev. E **56**, 7223 (1997).
[14] V. Tereshko and E. Shchekinova, Phys. Rev. E **58**, 423 (1998).
[15] D. Dangoisse, J.-C. Celet, and P. Glorieux, Phys. Rev. E **56**, 1396 (1997).
[16] V.N. Chizhevsky, Phys. Rev. E **64**, 036223 (2001).
[17] J.R. Tredicce, F.T. Arecchi, G.P. Puccioni, A. Poggi, and W. Gadomski, Phys. Rev. A **34**, 2073 (1986).